Osteoarthritis and Cartilage xxx (xxxx) xxx–xxx

Osteoarthritis and Cartilage

Proprioceptive role of the abductor pollicis longus in thumb carpometacarpal osteoarthritis: An anatomical and immunohistochemical study

C. Lamas [a b * 1], J. Serra [a b 2], M. Fa-Binefa [a b 3], E. Ramirez-Bermejo [a b 4], R. Orellana [b c 5], M. Garcia-Elias [d 6], A.L. Ladd [e 7]

[a] Department of Orthopaedic Surgery, Hospital de la Santa Creu i Sant Pau, Universitat Autònoma de Barcelona, Barcelona, Spain
[b] Musculoskeletal Research Group, Sant Pau Research Institute (IR Sant Pau), Barcelona, Spain
[c] Department of Pathology, Hospital de la Santa Creu i Sant Pau, Universitat Autònoma de Barcelona, Barcelona, Spain
[d] Institut Kaplan, Barcelona, Spain
[e] Robert A. Chase Hand and Upper Limb Center, Department of Orthopaedic Surgery, Stanford University, Stanford, California, USA

ARTICLE INFO

Article history:
Received 13 August 2025
Accepted 9 April 2026

Keywords:
Thumb
Carpometacarpal
Osteoarthritis
Osteophytes
Proprioception
Abductor Pollicis Longus

ABSTRACT

Objective: Thumb carpometacarpal (CMC) osteoarthritis (OA) is multifactorial and may involve anatomical variability, altered biomechanics, joint laxity and impaired proprioception. We hypothesized that variability of the abductor pollicis longus (APL) tendon and proprioceptive innervation of its insertions are associated with structural degeneration in thumb CMC OA, including cartilage degeneration and osteophyte area.
Design: In this cross-sectional study, twenty fresh-frozen cadaver hands were dissected (mean age 68 years, range 53–95) between June 2022 and December 2023. Anatomical and immunohistochemical analyses were performed using hematoxylin-eosin and alcian blue staining. Protein gene product 9.5 (PGP 9.5) and S-100 (glial marker) immunostaining were assessed. Macroscopic cartilage degeneration was graded using the International Cartilage Research Society (ICRS) classification, and histological degeneration was evaluated using Mankin and Otte scores. Associations between APL tendon morphology, cartilage degeneration and immunohistochemical findings were explored using non-parametric tests.
Results: Accessory APL tendinous slips were present in 18/20 (90%) specimens, with 3–6 slips identified per specimen. APL slip number showed weak inverse correlation with OA severity at the trapezium (r = −0.24 [−0.61, 0.22]), weak positive correlation with OA severity at MC1 (r = 0.14 [−0.31, 0.55]), moderate positive correlation with cartilage cellularity (r = 0.47 [0.04, 0.76]), weak positive correlation with Mankin score (r = 0.27 [−0.20, 0.63]), and weak positive correlation with Otte score (r = 0.36 [−0.10, 0.69]). S-100 status showed a moderate inverse association with OA severity at MC1 (r = −0.52 [−0.78, −0.10]).
Conclusions: Greater APL slip number was associated with increased cartilage cellularity, consistent with a more cellular cartilage phenotype in specimens with higher APL anatomical complexity. The inverse relationship between S-100 status and MC1 OA severity supports a potential role of innervation-related factors in structural degeneration. However, all analyses were unadjusted, and confounding by age cannot be excluded.

* Correspondence to: Hand Unit and Upper Limb, Department of Orthopaedic Surgery, Hospital de la Santa Creu i Sant Pau, Universitat Autonoma de Barcelona, Musculoskeletal Research Group, Sant Pau Research Institute (IR Sant Pau), Sant Quintí 77-79, Barcelona 08041, Spain.
E-mail addresses: clamasg@santpau.cat (C. Lamas), julia.serra14@gmail.com (J. Serra), Mfa@santpau.cat (M. Fa-Binefa), ERamirezBe@santpau.cat (E. Ramirez-Bermejo), Rorellana@santpau.cat (R. Orellana), Marc@garcia-elias.cat (M. Garcia-Elias), alad@stanford.edu (A.L. Ladd).
[1] ORCID: 0000-0001-7073-039X
[2] ORCID: 0009-0009-7079-898X
[3] ORCID: 0000-0001-5312-6975
[4] ORCID: 0000-0002-4770-1109
[5] ORCID: 0000-0003-1260-7064
[6] ORCID: 0000-0001-8815-3279
[7] ORCID: 0000-0003-0948-1034

https://doi.org/10.1016/j.joca.2026.04.007

Introduction

Studies have evaluated the role of nerve endings in the stabilizing structures of joints, mainly the knees and ankles [1–4]. Those studies have shown that some ligaments and stabilizing structures in those joints provide static stability and contribute to dynamic joint stability. In the upper limbs, Vangsness et al. [5] found that the coracoacromial ligament has sensory innervation. Moreover, patients with chronic shoulder pain presented altered innervation patterns. Hagert et al. [6] found sensory corpuscles and nerve fascicles in the scapholunate interosseous ligament (SLIL), suggesting that the SLIL may play a role in proprioception. The presence of Golgi corpuscles and nerve endings in other anatomical structures indicates that this structure is richly innervated and involved in hand proprioception [7]. More recently, Rein et al. mapped sensory nerve endings in the triangular fibrocartilage complex and showed that most components are richly innervated and contribute to neuromuscular stability of the distal radioulnar joint, whereas the articular disc and ulnolunate ligament are sparsely innervated and mainly mechanical stabilizers [8].

Thumb carpometacarpal (CMC) osteoarthritis (OA) is hypothesized to be associated with poor neuromuscular capacity and proprioceptive deficits [9]. The loss of dynamic and static stability leads to the progression of imbalance and functional deformity [9,10]. An increase in thumb CMC joint laxity and reduced proprioception have been associated with the development of thumb CMC OA [10–12]. In addition, clinical trials have shown that neurodynamic and joint mobilization techniques targeting the median or radial nerve and the CMC joint can transiently reduce pain sensitivity and, in some cases, improve grip strength in patients with thumb CMC OA, supporting a modulatory role of sensorimotor pathways in this joint [13–15].

Zancolli analyzed the biomechanical characteristics of the basal joint of the thumb and the joint overload generated by the presence of accessory tendons of the abductor pollicis longus (APL) and presented a surgical procedure consisting of tenotomy of the APL accessory tendons to unload the early OA of the thumb CMC joint [16]. Anatomical studies have shown that the APL frequently presents multiple tendinous slips and accessory insertions, not only to the first metacarpal (MC1) but also to the trapezium, joint capsule and thenar musculature [12,17]. These slips may act as a radial traction pulley, increasing shear forces across the CMC joint, promoting joint incongruence and favouring focal cartilage overload, osteophyte formation and progressive instability [16,18]. Despite these biomechanical hypotheses, the relationship between APL slip anatomy, the structural severity of thumb CMC osteoarthritis and the proprioceptive innervation of these insertions remains poorly characterized.

The aim of this study was to examine whether anatomical variability of the APL tendon and proprioceptive innervation of its insertions are associated with cartilage degeneration and osteophyte formation in the thumb CMC joint.

Methods

The cross-sectional study was carried out from June 2022 to December 2023. The study was approved by the institutional review board at our hospital (approval code: IIBSP-CMC-2022–69) and registered at ClinicalTrials.gov (NCT05626192). This study has been designed following the STROBE guidelines for observational studies.

Anatomical study: specimens, dissection technique and measurements

Twenty fresh-frozen cadaver hands from body donors were dissected at our anatomy department. Specimens were obtained from the institutional body donation program. Inclusion criteria were adult donors with an intact forearm and hand suitable for dissection. According to institutional policy, cadavers with known pre-existing systemic degenerative, inflammatory, neoplastic or traumatic conditions affecting the upper limb are not accepted for anatomical research; consequently, donors with documented systemic or degenerative diseases were excluded. All specimens were stored at −18 °C and used within one month of arrival to minimize tissue degradation and preserve histological and immunohistochemical integrity. Donor identification and detailed clinical histories are held by the Anatomy Department but are not accessible to the research team, in accordance with national privacy and ethical regulations. Each donor contributed a single hand (either right or left), so the 20 specimens (11 right, 9 left) were analyzed as independent observations rather than paired limbs. Dissection was performed with standard hand surgical instruments at a loupe magnification of 3.5x. Soft tissues over the first and second compartments were resected. The APL and extensor pollicis brevis (EPB) tendons and the thenar muscles were dissected. Sample size was determined pragmatically as an exploratory study by the number of eligible cadaveric specimens available. We examined the APL accessory tendons and attachments in the thenar muscles, the MC1, trapezium, EPB, opponens pollicis (OP) belly muscle, and joint capsule (Figure 1A). In all cases, we examined the joint surface and measured the dorsal-volar and radioulnar diameters of the trapezium and of the base of the MC1 using a digital caliper. The articular ‘contact area’ for each surface was then approximated as the product of these two orthogonal diameters, providing an estimated projected surface area rather than a direct 3D planimetric measure. The cartilage of the thumb CMC joint was examined macroscopically (Figure 1B). For each specimen, the trapezial and metacarpal articular surfaces were graded globally according to the highest ICRS grade observed on that surface, without formal subdivision into regional sectors. Cartilage degeneration was classified according the International Cartilage Research Society (ICRS) [19–21] criteria into five grades (0–4) [20] based on the depth and extent of the damage, as follows: grade 0: healthy cartilage with normal histologic morphology; grade I: nearly normal cartilage with superficial lesions, soft indentation and/or superficial fissures and cracks; grade 2: abnormal cartilage with moderate degeneration; lesions extending down to < 50% of cartilage depth; grade 3: severely abnormal with cartilage defects extending beyond > 50% of cartilage depth (3A) or down to the calcified layer (3B), or down to (but not through) the subchondral bone (3 C), with the presence of blisters (3D); grade 4: severely abnormal; complete cartilage loss with exposed subchondral bone [20,21]. For the purposes of this study, structural thumb CMC osteoarthritis was defined morphologically, based on the combination of macroscopic ICRS grades ≥ 2, histological degeneration compatible with OA (Mankin and Otte scores in the degenerative range) [22–24] and the presence of osteophytes and/or enthesophytes at the CMC joint.

The size and location of the main osteophytes in the thumb CMC joint were measured as absolute areas using a digital caliper (accuracy 0.01 mm, Tacklife Inc. DC010 150 mm/0–6; New York, USA).

Histology and immunohistochemistry

The APL accessory tendon insertion into the trapezium and the enthesophytes were harvested, fixed in 10% neutral buffered formalin, embedded in paraffin blocks, and sectioned into consecutive slices (3 µm). Sectioning was performed on a Leica Histocore Autocut rotary microtome (Leica Biosystems; Nussloch, Germany). The sections were then dehydrated and mounted on microscope slides. All immunohistochemical sections were evaluated by a single experienced musculoskeletal pathologist who was blinded to the

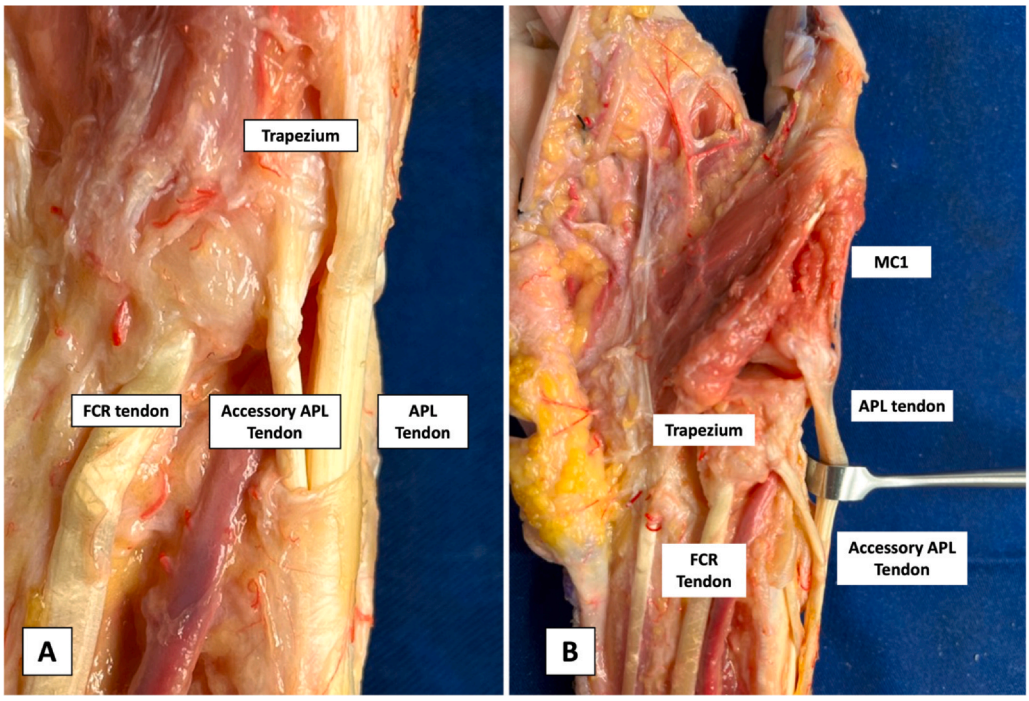

Fig. 1 Osteoarthritis and Cartilage

A) Thumb CMC joint showing the accessory APL tendon insertion in the trapezium. B) Thumb CMC joint with chondromalacia and OA. Abbreviations: FCR, flexor carpi radialis; APL, abductor pollicis longus tendon; Accessory APL tendon. accessory abductor pollicis longus; MC1, first metacarpal.

macroscopic cartilage grading, osteophyte measurements and APL anatomical findings at the time of assessment.

Staining was performed with hematoxylin and eosin (HE), Harry's hematoxylin, and a commercial eosin in an automated H&E stainer (Dako CoverStainer; Agilent Technologies; USA) to allow for assessment of tissue morphology. Alcian blue (AB) staining was performed with a commercial kit using an automated stainer (Arisant; Agilent Technologies) to determine the amount of proteoglycan synthesis as a reaction to degenerative changes. Histologic examination of the stained tissue sections was performed using a Leica light microscope (Leitz DMRB; Leica Biosystems Nussloch, Germany) at magnifications of 10x, 20x and 40x.

To perform the immunohistochemical analysis, we used a general nerve marker protein (protein gene product 9.5 (PGP 9.5), undiluted) from Novocastra Laboratories (Newcastle, UK) and the S-100 (dilution: 1:50) polyclonal antibodies from Dako-Agilent (Denmark), the two most reliable methods of detecting mechanoreceptors [2,6]. Tissue sections were paraffin-embedded and evaluated using an automated OMNIS immunostainer (Dako-Agilent; California, USA) followed by antibody detection using the Dako EnVision+System and 3,3´-diaminobenzidine as a chromogen. Appropriate positive and negative tissue controls were used throughout. Samples were classified as positive when any specific staining for S-100 or PGP 9.5 was detected, and as negative when no immunoreactivity was observed in the entire section.

The following characteristics were evaluated: matrix fissures, articular surface integrity, cell size, cell density, transition line between normal and calcified cartilage, vascularization, scar tissue, fibroblast proliferation, granulation tissue, hyalinization, chondroid metaplasia, calcification, ossification and loss of proteoglycans (Figure 2 A-G). The histopathological classification developed by Mankin was used to grade abnormalities in the articular cartilage [22,23] and then compared to the Otte grade [24] (Figure 3 A-D).

Mechanoreceptors were analyzed according to the Freeman and Wyke classification system [3,4], which classifies the receptors into four distinct types, as follows: type I (Ruffini endings); type II (Pacinian corpuscles); type III (Golgi-like endings); and type IV (free nerve endings).

Statistical analysis

The IBM-SPSS statistical software package v.29 was used to perform the statistical analysis. The main exposure variable was the number of APL tendon slips. The principal outcome variables were macroscopic cartilage degeneration (ICRS grade), histological degeneration (Mankin and Otte scores), cartilage cellularity per mm^3 and the presence or absence of S-100 and PGP 9.5 immunostaining. APL tendon slips, ICRS, Mankin and Otte scores were analysed as ordinal variables; cartilage cellularity, osteophyte area and linear bone measurements (e.g. distances, contact areas) were analysed as continuous variables; S-100 and PGP 9.5 were analysed as dichotomous variables (positive/negative). Given the small sample size and the predominantly ordinal nature of the main variables, all analyses were non-parametric. Continuous variables are presented as mean (SD) or median (IQR), according to distribution, categorical variables are presented as n (%).

Correlations between ordinal variables, or between ordinal and non-normally distributed continuous variables, were presented as Spearman's rho (r) with 95% confidence intervals (95% CIs). Comparisons of continuous or ordinal outcomes between dichotomous

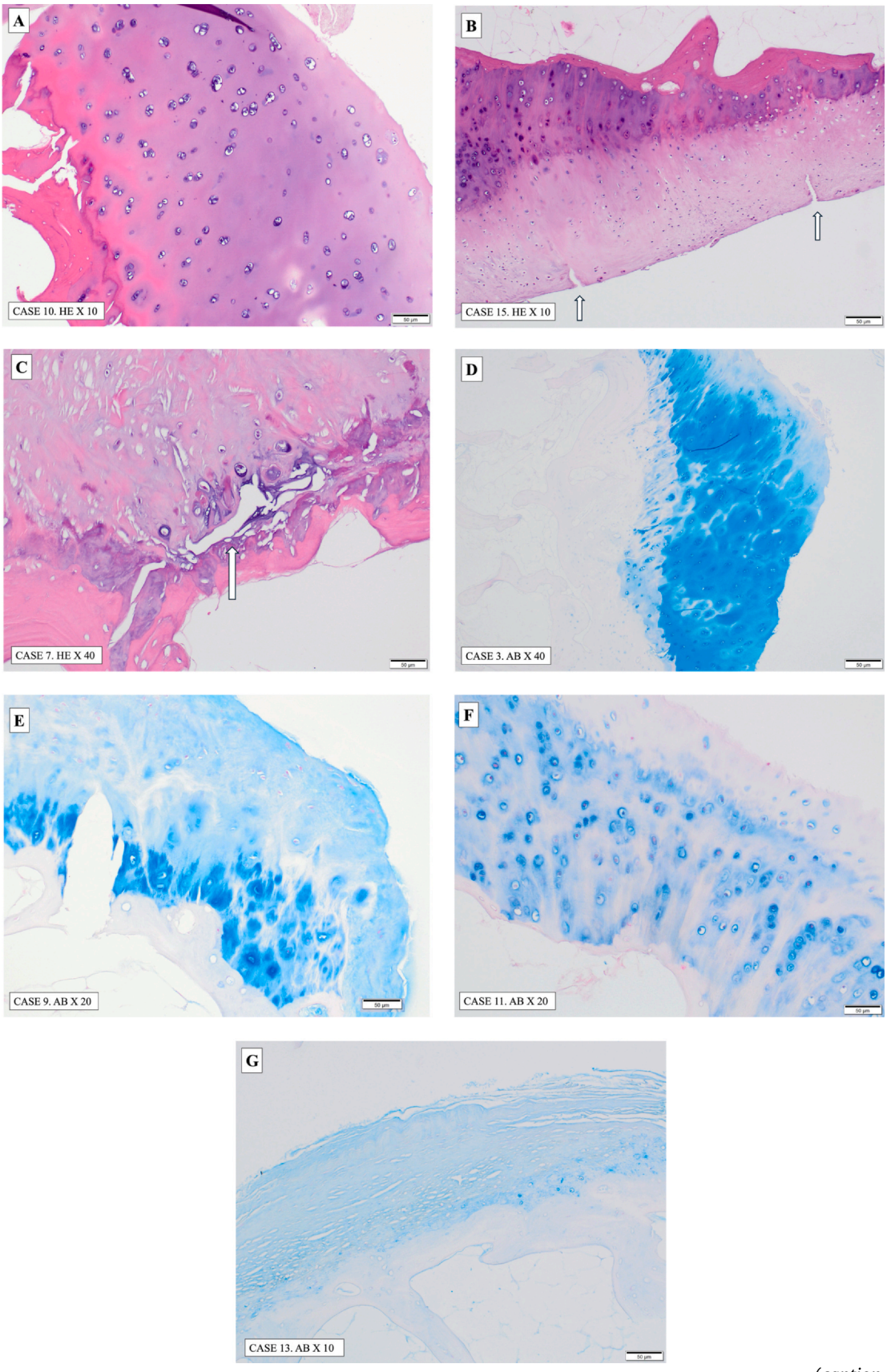

(caption on next page)

Fig. 2 Osteoarthritis and Cartilage

Progression of cartilage degeneration. Hematoxylin-eosin staining (HE): A) normal cartilage surface with normal chondrocytes distribution; B) superficial fissures on the surface and loss of water in the cellular matrix, with more chondrocytes per mm^2; C) deep fissures in the cartilage surface and almost no cells. The arrow indicates the fissures in the cartilage surface. Alcian blue staining (AB) shows the progression of proteoglycans loss in the same cartilage surface; D) normal quantity, deeply blue stained; E) slight loss of proteoglycans; F) Moderate loss of proteoglycans and G) severe loss of proteoglycans.

groups (e.g. S-100 positive vs. negative) were performed using the independent-samples Mann–Whitney U test, and results are presented as effect size r, calculated from the standardized Mann–Whitney statistic ($r = Z/\sqrt{N}$), with approximate 95% CIs derived using the Fisher r-to-z transformation.

Results

Anatomical analysis of APL attachments

The study included 20 human cadaveric hands (13 female, mean age, 68 years, range, 53–95), comprising 11 right hands and 9 left hands. The APL tendon inserted on the MC1 bone was the main tendon of the APL muscle.

We found a total of 47 tendons originating from the APL muscle (main and accessory). In half cases (n=10/20; 50%), the main APL tendon was divided into two independent tendons. In the remaining cases (n=10/20; 50%), there was either a single tendon (n=2, 10%), three (n=7; 35%) or four (n=1, 5%) tendons. These anatomical variants corresponded to the tendons originating in the APL muscle and extending to their insertion at the base of MC1. Overall, accessory APL slips (more than one insertion tendon) were present in 18 of the 20 specimens (90%). In ten specimens (n=10, 50%), the main APL tendon split into two tendinous slips before the insertion. In 19 cases (n=19, 95%) the main APL tendon was also inserted into the OP muscle belly and the abductor pollicis brevis (APB) muscle through these tendinous slips. The number of tendon slips from the APL tendon ranged from three to six, with 3 (n=9, 45%) and 4 (n=6, 30%) slips being the most frequent.

The APL tendon inserted into the MC1, occupying an area of 4.15 (IQR 3.3–6.0) mm^2. The number of APL tendon slips showed a moderate positive correlation with cartilage cellularity (r = 0.47 [0.04, 0.76]), indicating that specimens with more slips tended to present higher chondrocyte cellularity.

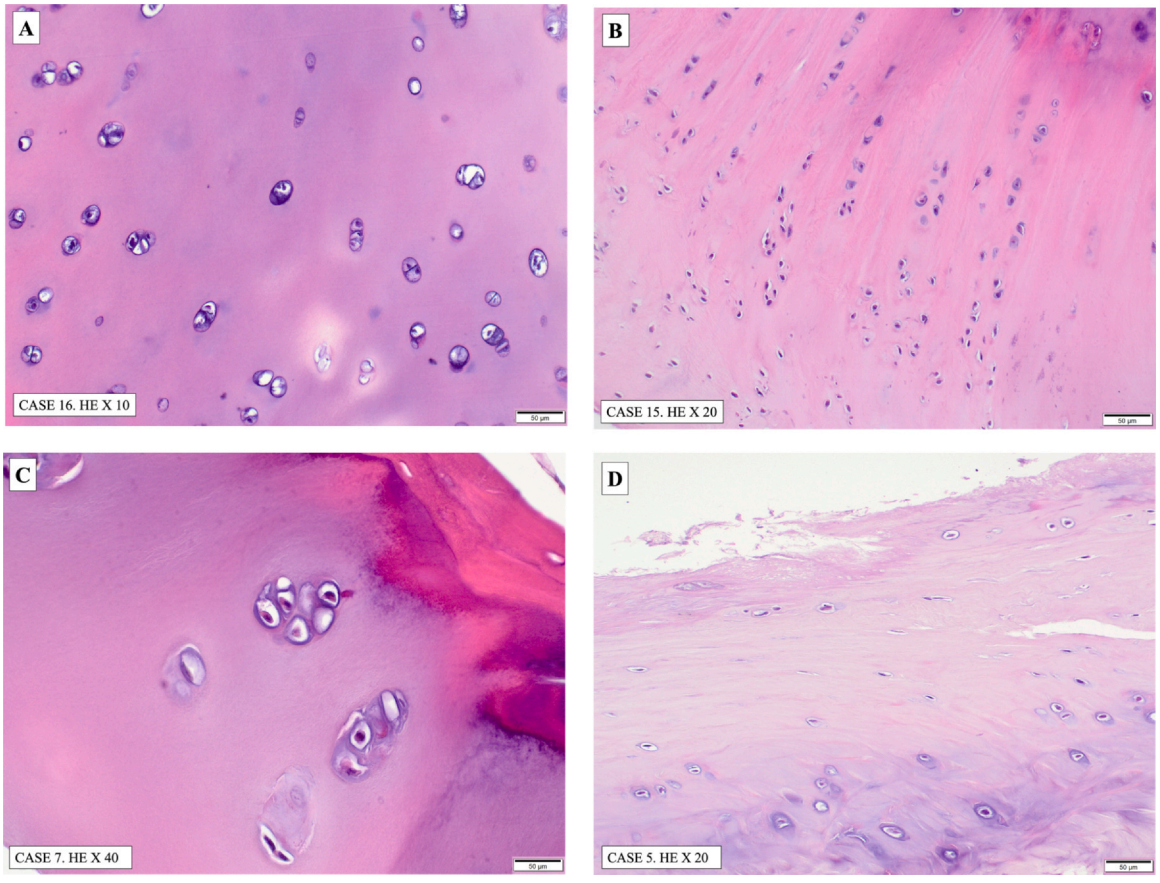

Fig. 3 Osteoarthritis and Cartilage

Cellularity gradient on hematoxylin-eosin staining (HE) from: A) normal cellularity, B) cellularity slightly increased, C) chondrocyte clones in the initial phases of OA, and D) decrease in chondral cellularity.

The radial osteophytes were larger, on average, than the ulnar osteophytes (8.39 ± 1.67 vs. 3.91 ± 2.37 mm^2). Larger radial and ulnar osteophyte area showed moderate correlations with histological outcomes, including cartilage cellularity (radial r = 0.36 [-0.10, 0.69]; ulnar r = 0.36 [-0.10, 0.69]), global Mankin score (radial r = 0.34 [-0.12, 0.68]; ulnar r = 0.28 [-0.17, 0.64]), and Otte score (radial r = 0.32 [-0.14, 0.66]; ulnar r = 0.34 [-0.12, 0.68]).

The first compartment septum was present in four specimens (n=4, 20%). In the remaining specimens (no septum), the distance from the first extensor retinaculum to the MC1 and to the trapezium were, respectively, 24.1 mm (IQR 20.2–29.3) and 19.0 mm (IQR 15.0–22.9). The presence of a septum between APL and EPB showed a trend toward lower OA grade at MC1 (r = −0.41 [-0.71, 0.06]).

The grade of cartilage damage (ICRS) on the metacarpal surface was 3–4 versus 2–3 on the trapezium. Trapezium articular surface area showed moderate correlation with histological outcomes, including cartilage cellularity (r = 0.36 [-0.09, 0.69]), global Mankin score (r = 0.25 [-0.22, 0.63]), and Otte score (r = 0.29 [-0.17, 0.65]). Insertion into the deep capsule and into the opponens muscle belly showed small positive correlations with OA severity and histological outcomes (r = 0.16–0.31). Insertion footprint areas at MC1 and the trapezium, as well as APL tendon area, demonstrated weak associations with OA and cartilage histology (approximately r = −0.35 to 0.33). Distances from the first extensor compartment to MC1 and the trapezium showed weak-to-moderate trends with cartilage cellularity, such as the inverse association observed for the first extensor compartment–MC1 distance (r = −0.38 [−0.70, 0.08]). The anatomical measures are shown in Table 1 and the correlations in Table 2. Overall, APL slip number showed the strongest relationship with histological cartilage cellularity, while S-100 status was primarily related to MC1 structural OA severity. Plots of the main exposure versus the principal outcomes are shown in Supplementary Material 1.

Histological and immunohistochemical analysis of the thumb CMC joint

The median Mankin score was 9 (IQR 6.5–11) and the median Otte score was 3 (IQR 1.75–4). Overall, the majority of specimens showed structural degeneration compatible with moderate to severe CMC osteoarthritis, with ICRS grades ≥ 2 in both the trapezial and metacarpal surfaces in all joints (20/20, 100%). Of the 20 specimens, 13 (4 males, 9 females) tested positive for S-100 (Figure 4 A-D).

The specimens that exhibited greater degenerative arthropathy and cartilage loss presented fewer nerve terminals and a negative S-100 marker (Figures 5A and 5B). Two specimens tested positive for PGP 9.5.

S-100 status demonstrated a moderate inverse correlation with OA severity at MC1 according to the ICRS classification (r = −0.52 [−0.78, −0.10]). Correlations between S-100 status and histological outcomes were weak, including cartilage cellularity (r = −0.08 [−0.51, 0.38]), global Mankin score (r = −0.07 [−0.50, 0.38]), and Otte score (r = −0.19 [−0.58, 0.28]) (Figure 6).

The histological and immunohistochemical analysis measures are shown in Table 1 and the correlations in Table 2. No multivariable analyses were performed and all reported associations are unadjusted and may be affected by residual confounding.

Anatomical Analysis					
Number of APL slips (*number of slips*, n, (%))					
3	*4*	*5*	*6*		
9 (45)	6 (30)	4 (20)	1 (5)		
Number of APL Slips – MC1 (*number of slips*, n,(%))					
1	*2*	*3*	*4*		
2 (10)	10 (50)	7 (35)	1 (5)		
Number of APL slips – Trapezium (*number of slips*, n, (%))					
0	*1*	*2*	*3*		
1 (5)	16 (80)	2 (10)	1 (5)		
Insertion into deep capsule (n, (%))					
16 (80)					
Insertion into OP (n, (%))					
19 (95)					
Surface MC1 insertion (median mm2, (IQR))					
4.15 (3.3–6.0)					
Dimension APL tendon (median mm2 ICRS, (IQR))					
5.25 (4.6–6.2)					
Distance 1st EC-MC1 (median mm ICRS, (IQR))					
24.1 (20.2–29.3)					
Distance 1st EC-trapezium (median mm ICRS, (IQR))					
19.0 (15.0–22.9)					
Septum between APL-EPB (n, (%))					
4 (20)					
Articular surface MC1 (mean mm2 ICRS, (SD))					
11.95 (3.0)					
Articular surface trapezium (mean mm2 ICRS, (SD))					
12.67 (2.9)					
Radial osteophyte dimension (mean mm ICRS, (SD))					
8.39 (1.67)					
Ulnar osteophyte dimension (median mm ICRS, (IQR))					
3.91 (2.25–4.68)					
Histology - Immunohistochemical analyses					
OA trapezium ICRS classification (*OA trapezium ICRS*, n, (%))					
2	*3*	*4*			
4 (20)	7 (35)	9 (45)			
OA MC1 ICRS classification (*OA MC1 ICRS*, n, (%))					
2	*3*	*4*			
6 (30)	10 (50)	4 (20)			
Overall Mankin classification (*Mankin Classification*, n, (%))					
2	*3*	*4*	*5*	*6*	*7*
2 (10)	1 (5)	1 (5)	1 (5)	0 (0.0)	1 (5)
8	*9*	*10*	*11*	*12*	*13*
0 (0.0)	2 (10)	3 (15)	6 (30)	2 (10)	1 (5)
Cartilage cellularity (Mankin classification) (*Mankin classification*, n, (%))					
0	*1*	*2*	*3*		
2 (10)	4 (20)	2 (10)	12 (60)		
Overall Otte classification (*Otte classification*, n, (%))					
0	*1*	*2*	*3*	*4*	
2 (10)	3 (15)	1 (5)	8 (40)	6 (30)	
S-100 marker (n, (%))					
13 (65)					
PGP 9.5 marker (n, (%))					
2 (10)					

Abbreviations: APL = Abductor pollicis longus; MC1 = First Metacarpal bone; OP = Opponens; EC = Extensor compartment; EPB = Extensor pollicis brevis; ICRS = International Cartilage Research Society, SD = Standard Deviation, IQR = Interquartile range

Table 1 Osteoarthritis and Cartilage

Anatomical and immunohistochemical baseline data.

Discussion

Our findings confirm the anatomical variability of the APL tendon. Accessory tendinous slips were present in 75% of the specimens (15 cases), inserting into the MC1, deep joint capsule, trapezium and thenar muscles (APB and OP). The presence of these tendinous slips was positively correlated (Table 2) with higher cartilage cellularity per mm^3.

Histological and immunohistochemical analysis demonstrated that a greater degenerative change in the thumb CMC joint was associated with a lower expression of Golgi mechanoreceptors and reduced S-100 immunostaining and fewer nerve-related structures, indicating reduced proprioception in joints with severe cartilage loss. The radial osteophytes in the trapezium were larger on average than the ulnar osteophytes; this pattern is consistent with a trend toward asymmetric joint degeneration, but should be interpreted

	OA Trapezium (ICRS classification)	OA MC1 (ICRS classification)	Cartilage cellularity (Mankin classification)	Mankin	Otte
Number of APL slips	-0.24 (-0.61, 0.22)	0.14 (-0.31, 0.55)	**0.47 (0.04, 0.76)**	0.27 (-0.20, 0.63)	**0.36 (-0.10, 0.69)**
Number of APL slips – MC1	-0.02 (-0.45, 0.42)	0.17 (-0.33, 0.53)	0.34 (-0.12, 0.68)	0.18 (-0.28, 0.57)	0.20 (-0.26, −0.59)
Number of APL slips – Trapezium	-0.15 (-0.55, 0.31)	**0.38 (-0.08, 0.70)**	-0.20 (-0.59, 0.26)	-0.16 (-0.56, 0.30)	-0.24 (-0.61, 0.22)
Insertion into deep capsule*	0.19 (-0.27, 0.59)	0.25 (-0.21,-0.63)	-0.02 (-0.46, 0.42)	0.21 (-0.25, 0.60)	0.31 (-0.15, 0.66)
Insertion into OP*	0.23 (-0.24, 0.61)	0.04 (-0.41, 0.48)	0.18 (-0.29, 0.57)	0.16 (-0.31, 0.56)	0.29 (-0.18, 0.65)
Area MC1 insertion	**0.33 (-0.13, 0.67)**	0.13 (-0.33, 0.53)	-0.06 (-0.48, 0.39)	-0.17 (-0.56, 0.29)	-0.07 (-0.49, 0.38)
Area trapezium insertion	-0.12 (-0.53, 0.33)	-0.04 (-0.47, 0.40)	-0.07 (-0.49, 0.37)	-0.13 (-0.53, 0.33)	-0.05 (-0.47, 0.39)
Area APL tendon	**-0.35 (-0.68, 0.11)**	-0.01 (-0.44, 0.43)	-0.07 (-0.49, 0.37)	-0.20 (-0.58, 0.26)	-0.15 (-0.55, 0.30)
Distance 1st EC – MC1	-0.27 (-0.64, 0.18)	-0.03 (-0.46, 0.40)	**-0.38 (-0.70, 0.08)**	-0.19 (-0.58, 0.27)	-0.23 (-0.60, 0.23)
Distance 1st EC – trapezium	0.03 (-0.41, 0.46)	0.06 (-0.39, 0.48)	-0.17 (-0.56, 0.29)	0.02 (-0.42, 0.45)	-0.11 (-0.52, 0.34)
Septum between APL-EPB*	**-0.32 (-0.66, 0.14)**	**-0.41 (-0.71, 0.06)**	0.02 (-0.42, 0.46)	-0.02 (-0.46, 0.42)	-0.01 (-0.44, 0.43)
Articular surface MC1	-0.31 (-0.66, 0.15)	-0.08 (-0.50, 0.37)	0.01 (-0.42, 0.44)	-0.05 (-0.47, 0.39)	0.03 (-0.41, 0.45)
Articular surface trapezium	-0.03 (-0.46, 0.40)	0.20 (-0.26, 0.59)	**0.36 (-0.09, 0.69)**	0.25 (-0.22, 0.63)	0.29 (-0.17, 0.65)
Radial osteophyte dimension	-0.08 (-0.50, 0.37)	-0.13 (-0.54, 0.32)	**0.36 (-0.10, 0.69)**	**0.34 (-0.12, 0.68)**	**0.32 (-0.14, 0.66)**
Ulnar osteophyte dimension	0.02 (-0.42, 0.45)	-0.06 (-0.48, 0.39)	**0.36 (-0.10, 0.69)**	0.28 (-0.17, 0.64)	**0.34 (-0.12, 0.68)**
S-100 marker*	-0.28 (-0.64, 0.19)	**-0.52 (-0.78, −0.10)**	-0.08 (-0.51, 0.38)	-0.07 (-0.50, 0.38)	-0.19 (-0.58, 0.28)

Values are presented as Spearman's rho (95% CI) for correlation analyses and as Mann–Whitney effect size r (95% CI) for dichotomous group comparisons (marked with *).
Bold: Moderate associations
Abbreviations: OA, osteoarthritis; MC1, first metacarpal bone; APL, abductor pollicis longus; OP, opponens pollicis: EPB, extensor pollicis brevis (EPB); ICRS, International Cartilage Research Society; EC, extensor compartment.

Table 2 Osteoarthritis and Cartilage

Anatomical and immunohistochemical data analyses.

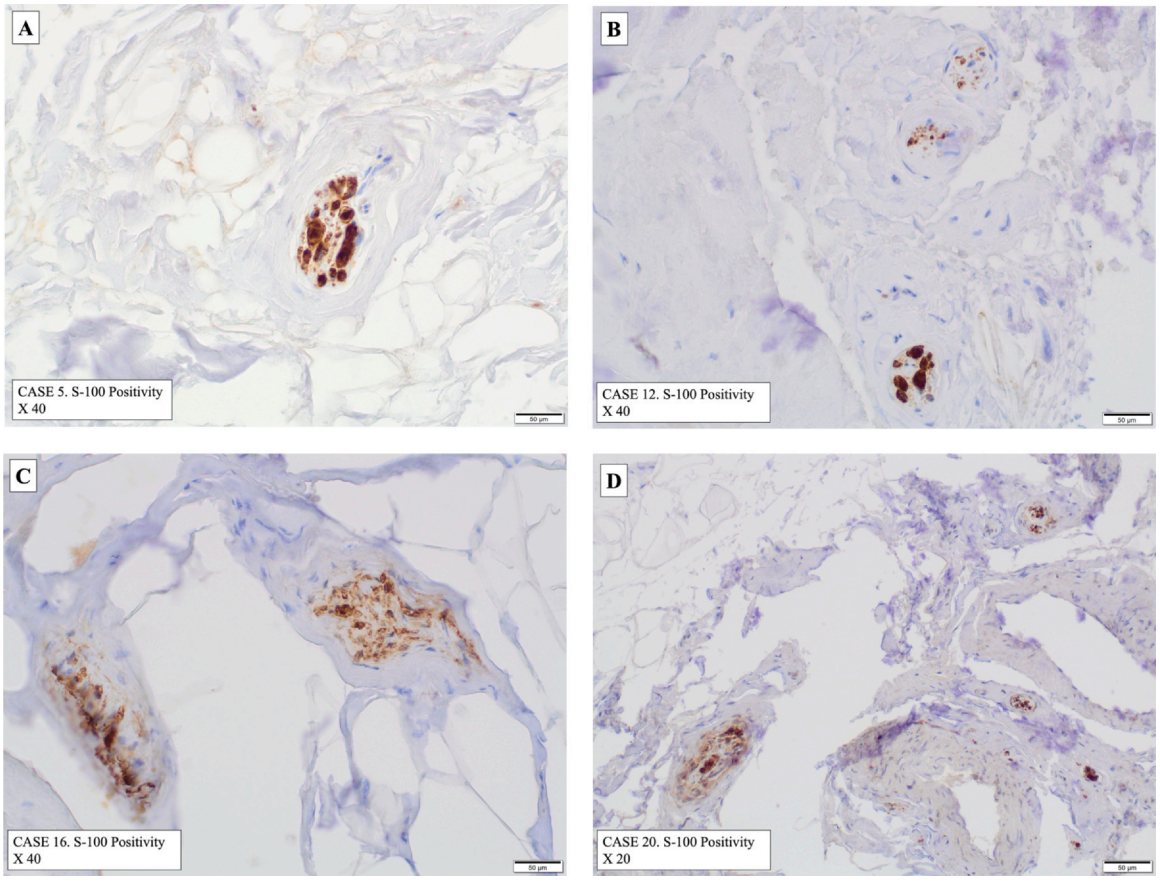

Fig. 4 Osteoarthritis and Cartilage

A-D: Cases with S-100 marker positivity (x 40, x20).

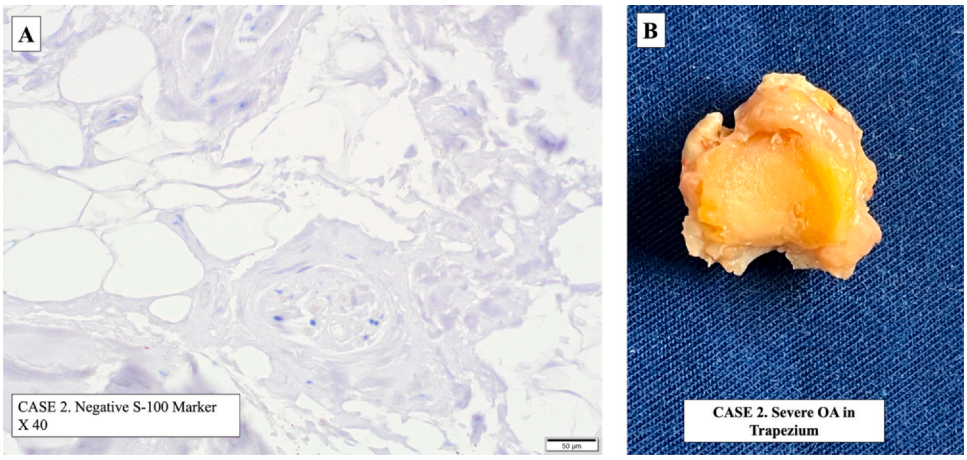

Fig. 5 Osteoarthritis and Cartilage

Case 2: A) Negative S-100 marker x40 associated with B) Severe OA in trapezium bone; ICRS Grade 3: severely abnormal, cartilage defects extending down > 50% of cartilage depth.

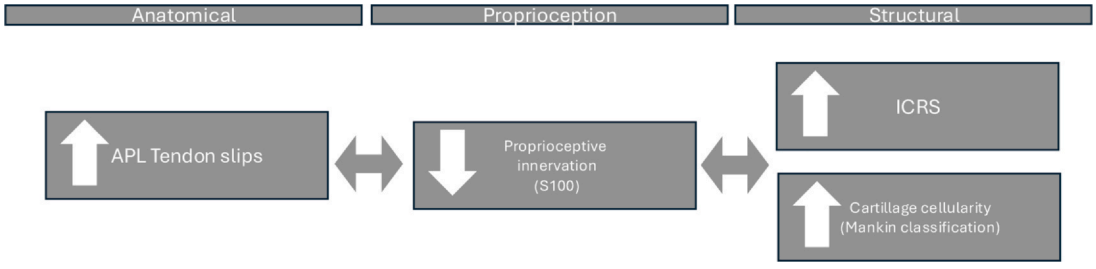

Fig. 6 Osteoarthritis and Cartilage

Diagram representing the different phases of the study: anatomical, proprioceptive, and structural.

with caution. Our observations are in line with previous quantitative mapping studies of thumb CMC OA reporting that cartilage thinning on the thumb metacarpal tends to initiate in the radial quadrants and progress towards the volar regions, whereas on the trapezium early thinning appears in the radial and dorsal-radial quadrants, with subsequent involvement of volar areas in late stages of disease [25].

The findings of this study are consistent with previous reports describing anatomical variability in the APL, including accessory insertions, with the potential biomechanical implications [12,22–24,26–28]. This aligns with prior observations that cartilage injury may be accompanied by increased cellularity [23,24].

The instability of the saddle-shaped thumb CMC joint has long been recognized as a contributing factor to the development of OA [16–18,29]. Some authors emphasize the role of repetitive mechanical overload, hormonal influences, dysplasia, structural damage, and/or ligamentous laxity as primary factors in thumb CMC OA [17,30,31]. However, other authors suggest that the thumb CMC joint should be viewed as a synovial organ, where all joint components contribute to the pathogenesis of OA [10,29]. In this cohort, several anatomical insertion patterns (deep capsule and opponens muscle belly) demonstrated only small, inconsistent relationships with OA severity and histological degeneration, indicating no clear association between these insertion variants and the degenerative phenotype.

Zancolli have suggested that biomechanical factors such as the presence of a septum between the APL and EPB in the first extensor compartment and the distance between the first extensor compartment and the MC1 or trapezium may increase traction-pulley radial force, joint incongruence, and uneven cartilage loading, thereby accelerating degeneration [16–18]. In our sample, the presence of a septum between APL and EPB showed a trend toward lower OA severity at MC1, although the uncertainty was substantial and no definitive association can be established. Likewise, spatial measures (distances from the first extensor compartment to MC1 and trapezium) showed weak-to-moderate trends with cartilage cellularity, but no confirmed relationship with cartilage degeneration can be concluded.

Early OA has been associated with enthesopathy-related osteophyte area [30–35], which is supported by the results of our study. All of the cadaveric specimens in our sample with moderate to severe OA exhibited osteophytes. Osteophyte area (radial and ulnar) demonstrated moderate correlations with cartilage cellularity, global Mankin score and Otte classification, suggesting a possible tendency for larger osteophytes to be linked to greater histological activity and degeneration, although the confidence intervals indicate substantial

imprecision. Similarly, trapezium articular surface area showed moderate correlations with histological outcomes, but the evidence remains weak and compatible with no true association.

The Golgi tendon organ, a key proprioceptive receptor, is responsible for transmitting information about movement and joint positioning [4,36,37]. Rein et al. suggested that differences in ligament innervation reflect functional differences, with non-innervated ligaments acting as passive stabilizers and richly innervated ligaments contributing to proprioception [8,36,37]. The immunohistochemical findings of this study provide additional insight into the role of proprioception in thumb CMC OA progression.

We used S-100 as a general neuronal marker to identify the presence of nerve-related structures, and observed that S-100 immunostaining tended to be reduced in specimens with more advanced degenerative changes, indicating a potential reduction in innervation. The inverse relationship between S-100 status and OA severity at MC1 could indicate a more preserved cartilage phenotype or differences in tissue maturation/innervation associated with S-100 expression. From a pathophysiological perspective, this reduction in proprioceptive afferents may contribute to mechanotransduction failure at the CMC joint, altering chondrocyte responses to load and disrupting the normal coupling between mechanical stimuli, neuromuscular control and cartilage metabolism that maintains joint homeostasis in earlier stages of disease. These findings are comparable to previous studies on ankle ligaments, in which free nerve endings were found to be the predominant type of sensory endings, followed by Ruffini endings [36]; by contrast, in the triangular fibrocartilage complex, mechanoreceptor distribution remains consistent across different specimens [8].

From a translational perspective, our structural and immunohistochemical findings are in line with clinical studies showing that targeted neurodynamic and joint mobilization techniques can modulate pain sensitivity and, in some cases, grip strength in patients with thumb CMC osteoarthritis [38]. Neurodynamic mobilization of the median or radial nerve and passive accessory mobilization of the CMC joint have been reported to produce short-term hypoalgesic effects and small improvements in grip strength, suggesting that sensorimotor pathways around the thumb CMC can be therapeutically influenced in vivo. [38–40]. In this context, the reduced expression of proprioceptive markers that we observed in joints with advanced structural degeneration supports the hypothesis that preserving or enhancing proprioceptive input may represent a complementary target—alongside purely biomechanical strategies—in early or moderate stages of thumb CMC OA.

This study has several limitations, including the cross-sectional study design. A second limitation is the use of cadaveric specimens, which restricts our ability to assess functional aspects of joint stability and proprioception. A third limitation is that we were unable to evaluate individual patient factors, such as occupational history, genetic predisposition, or prior joint trauma, even though those factors could contribute to variations in APL tendon anatomy and OA severity. Another limitation of this study was that only the APL tendon was analyzed in detail, despite the fact that other muscle–tendon units may also influence the biomechanics of the thumb CMC. Moreover, osteophyte area was analyzed as an absolute measure and not adjusted for trapezium or metacarpal size, which may partially confound the interpretation of osteophyte burden; future studies should consider size-normalised osteophyte indices or include bone size as a covariate. In addition, the study was based on a convenience sample, which further limits statistical power and the precision of our estimates. Finally, the absence of validated inter- and intra-observer reliability data for macroscopic and osteophyte measurements was also a limitation. In addition, we did not obtain standardized radiographs or perform Eaton–Littler or Kellgren–Lawrence grading, nor did we conduct micro-CT or HR-pQCT analysis of bone microarchitecture, as reported in previous work on trapezial and MC1 pathology; our definition of OA was therefore based exclusively on macroscopic, histological and osteophyte findings at the CMC joint [38–40]. Because detailed clinical histories and radiographic information were not available, we cannot determine whether the observed structural degeneration reflects primary idiopathic OA, age-related cartilage wear, prior localized trauma, or a combination of these factors; our findings should therefore be interpreted as degenerative changes compatible with osteoarthritis rather than as a clinically defined OA diagnosis. Given the cross-sectional design, modest sample size, and the fact that all analyses were unadjusted, the observed associations should be interpreted with caution. Residual confounding, particularly by age, cannot be excluded, and no causal inferences can be drawn regarding the relationship between APL tendon morphology, proprioceptive markers and thumb CMC osteoarthritis.

By contrast, an important strength of the study is the combination of anatomical, histological and immunohistochemical analyses, which may provide insights into the relationship between APL tendon anatomy, proprioception, and thumb CMC OA.

This study suggests that a greater number of APL tendon slips is associated with increased cartilage cellularity. In addition, the inverse association between S-100 and MC1 OA severity supports the concept that proprioceptive or innervation-related factors may contribute to joint degeneration, highlighting the relevance of considering both biomechanical and neurophysiological mechanisms in thumb CMC osteoarthritis However, the evidence was weak for the majority of outcomes and these findings should therefore be interpreted with caution.

Authors contribution

Conception and design: CL, MGE, ALL. Collection and assembly of data: CL, JS, MFB, RO, MGE, ALL; Analysis and interpretation of the data: CL, RO, MFB, ERB, MGE, ALL. Drafting of the article: CL; Critical revision of the article for important intellectual content: All authors; Final approval of the article: All authors.

Ethics approval

This study was approved by the hospital ethics committee: approval code: IIBSP-CMC-2022–69 v1 NCT 05626192.

Funding

There was no funding provided for this work.

Declaration of Competing Interest

The authors declare no competing interests.

Declaration of generative AI and AI-assisted technologies in the writing process

No AI tools have been used for writing this manuscript.

Acknowledgments

We thank the cadaver donors and their families. We would also like to thank A. Prats, Director of the Human Body Donation, and M. Llusà from the Department of Human Anatomy, Faculty of Medicine, for their indispensable contributions to this study. We also thank I. Gich from the Clinical Epidemiology Department for assistance with the statistical analysis and other contributions to this study. This work has been carried out within the framework of the Doctoral Program in Surgery and Morphological Sciences at the Universitat Autònoma de Barcelona.

Appendix A. Supporting information

Supplementary data associated with this article can be found in the online version at doi:10.1016/j.joca.2026.04.007.

References

[1] R.L. Barrack, H.B. Skinner, The sensory function of knee ligaments, in: D.M. Daniel, W.H. Akeson, J.J. Connor (Eds.), Knee ligaments: structure, function, injury and repair, Raven Press, New York, 1990, pp. 95–114.
[2] E. Hagert, B.O. Ljung, S. Forsgren, General innervation pattern and sensory corpuscles in the scapholunate interosseous ligament, Cells Tissues Organs 177 (2004) 47–54, https://doi.org/10.1159/000078427
[3] M.A. Freeman, B. Wyke, The innervation of the ankle joint: an anatomical and histological study in the cat, Acta Anat. 68 (1967) 321–333, https://doi.org/10.1159/000143037
[4] M.A. Freeman, B. Wyke, The innervation of the knee joint: an anatomical and histological study in the cat, J. Anat. 101 (1967) 505–532.
[5] C.T. Vangsness Jr, M. Ennis, J.C. Taylor, R. Atkinson, Neural anatomy of the glenohumeral ligaments, labrum and subacromial bursa, Arthroscopy 11 (1995) 180–184, https://doi.org/10.1016/0749-8063(95)90064-0
[6] E. Hagert, M. Garcia-Elias, S. Forsgren, B.O. Ljung, Immunohistochemical analysis of the wrist ligaments innervation in relation to their structural composition, J. Hand Surg. Am. 32 (2007) 30–36, https://doi.org/10.1016/j.jhsa.2006.10.005
[7] I. Garcia-Martínez, Y. Garcia-Mesa, J. Garcia-Piqueras, A. Martinez-Pubil, J.L. Cobo, J. Feito J, et al., Sensory innervation of the human palmar aponeurosis in healthy individuals and patients with palmar fibromatosis, J. Anat. 240 (2022) 972–984, https://doi.org/10.1111/joa.13609
[8] S. Rein, M. Semisch, M. Garcia-Elias, A. Lluch, H. Zwipp, E. Hagert, Immunohistochemical mapping of sensory nerve endings in the human triangular fibrocartilage complex, Clin. Orthop. Relat. Res. 473 (2015) 3245–3253, https://doi.org/10.1007/s11999-015-4357-z
[9] A.L. Ladd, A.P.C. Weiss, J.J. Crisco, E. Hagert, J.M. Woft, S.Z. Glickel, et al., The thumb carpometacarpal joint: anatomy, hormones and biomechanics, Instr. Course Lect. 62 (2013) 165–179.
[10] E. Hagert, J. Lee, A.L. Ladd, Innervation patterns of thumb trapeziometacarpal joint ligaments, J. Hand Surg. Am. 37 (2012) 706–714.e1, https://doi.org/10.1016/j.jhsa.2011.12.038
[11] H. Johnsson, S.T. Valrysdortir, O. Kjartansson, A. Brekkan, Hypermobility associated with osteoarthritis of the thumb base: a clinical and radiological subset of hand osteoarthritis, Ann. Rheum. Dis. 55 (1996) 540–543, https://doi.org/10.1136/ard.55.8.540
[12] A.L. Ladd, J. Lee, E. Hagert, Macroscopic and microscopic analysis of the thumb carpometacarpal ligaments. A cadaveric study of ligament anatomy and histology, J. Bone Jt. Surg. Am. 94 (2012) 1466–1477, https://doi.org/10.2106/JBJS.K.00329
[13] J.H. Villafañe, G.B. Silva, J. Fernandez-Carnero, Short-term effects of neurodynamic mobilization in 15 patients with secondary thumb carpometacarpal osteoarthritis, J. Manip. Physiol. Ther. 34 (2011) 449–456, https://doi.org/10.1016/j.jmpt.2011.05.016
[14] J.H. Villafañe, J.A. Cleland, C. Fernandez-de-Las-Peñas, Bilateral sensory effects of unilateral passive accessory mobilization in patients with thumb carpometacarpal osteoarthritis, J. Manip. Physiol. Ther. 36 (2013) 232–237, https://doi.org/10.1016/j.jmpt.2013.05.008
[15] J.H. Villafañe, M.D. Bishop, C. Fernández-de-Las-Peñas, D. Langford, Radial nerve mobilisation had bilateral sensory effects in people with thumb carpometacarpal osteoarthritis: a randomised trial, J. Physiother. 59 (2013) 25–30, https://doi.org/10.1016/S1836-9553(13)70143-7
[16] E.A. Zancolli, The trapeziometacarpal joint. Tenotomy of the accessory tendons in early osteoarthritis, Hand Clin. 17 (2001) 13–43.
[17] J. R. Opreanu, H. Wechter, J.P. Tabbaa, M. Kepros, Y. Baulch, Y. Xie, et al., Anatomic variations of the first extensor compartment and abductor pollicis longus tendon in trapeziometacarpal arthritis, Hand 5 (2010) 184–189, https://doi.org/10.1007/s11552-009-9234-3
[18] S. Gupta, H. Michelsen-Jost, Anatomy and function of the thenar muscles, Hand Clin. 28 (2012) 1–7, https://doi.org/10.1016/j.hcl.2011.09.006
[19] P. Mainil-Varlet, T. Aigner, M. Brittberg, P. Bullough, A. Hollander, E. Hunziker, et al., Histological assessment of cartilage repair: a report by the histology endpoint committee of the International Cartilage Repair Society (ICRS), J. Bone Jt. Surg. Am. 85 (2) (2003) 45–57.
[20] R.U. Kleemann, D. Kroker, A. Cedrano, J. Tuischer, G.N. Duda, Altered cartilage mechanics and histology in knee osteoarthritis: relation to clinical assessment (ICRS grade), Osteoarthr. Cartil. 13 (2005) 858–863, https://doi.org/10.1016/j.joca.2005.06.008
[21] R.E. Outerbridge, The etiology of chondromalacia patellae, J. Bone Jt. Surg. Br. 43 (1961) 752–757, https://doi.org/10.1302/0301-620X.43B4.752
[22] H.J. Mankin, H. Dorfman, L. Lippiello, A. Zarins, Biomechanical and metabolic abnormalities in articular cartilage from osteoarthritic human hips. II. Correlation of morphology with biochemical and metabolic data, J. Bone Jt. Surg. Am. 53 (1971) 523–537, https://doi.org/10.2106/00004623-197153030-00009
[23] S. Söder, T. Aigner, Arthrose. Etiology, typing, staging and histological grading, Pathologe 32 (2011) 183–192, https://doi.org/10.1007/s00292-011-1419-1
[24] T. Aigner, S. Söder, Histopathologische begutachtung der gelenkdegeneration, Pathologe 27 (2006) 431–438, https://doi.org/10.1007/s00292-006-0864-8
[25] M.F. Koff, O.F. Ugwonali, R.J. Strauch, M.P. Rosenwasser, G.A. Ateshian, V.C. Mow, Sequential wear patterns of the articular cartilage of the thumb carpometacarpal joint in osteoarthritis, J. Hand Surg. Am. 28 (2003) 597–604, https://doi.org/10.1016/s0363-5023(03)00145-x
[26] J. Martí-Gorreto, M. San-Millán, A. Carrera, R.Share Tubbs, J. Iwanaga, A. Cateura, et al., The anatomy of the tendon of abductor pollicis longus and its morphological variations: an anatomical approach emphasizing the clinical relevance, Ann. Anat. 247 (2023) 1–10, https://doi.org/10.1016/j.aanat.2023.152068
[27] D.S. Shah, C. Middleton, S. Gurdezi, M.D. Horwitz, A.E. Kedgley, The importance of abductor pollicis longus in wrist motions: a physiological wrist simulator study, J. Biomech. 77 (2018) 218–222, https://doi.org/10.1016/j.jbiomech.2018.07.011
[28] C.W. Moore, J. Fanous, C.L. Rice, Fiber type composition of contiguous palmaris longus and abductor pollicis brevis muscles: morphological evidence of a functional synergy, J. Anat. 238 (2021) 53–62, https://doi.org/10.1111/joa.13289
[29] S. Deivasigamani, A. Azad, S.S. Yang, The variable insertional anatomy of the abductor pollicis longus: functional relevance and relationship to adjacent thumb extensors, Hand 18 (2023) 145–152, https://doi.org/10.1177/15589447219997 34
[30] C. Lamas-Gomez, A.M. Gondolbeu, R. Morro-Marti, I. Proubasta-Renart, M. Llusa-Perez, The role of the carpometacarpal ligaments of the thumb in stability and the development of osteoarthritis lesions: an anatomical study, Acta Orthop. Belg. 83 (2017) 449–457.
[31] F.B.P. Kroon, S. Van Beest, S. Ermulat, M.C. Kortekaas, J.L. Bloem, M. Reijnierse, et al., thumb base osteoarthritis structural damage is more strongly associated with pain and synovitis, Osteoarthr. Cartil. 26 (2018) 1196–1202, https://doi.org/10.1016/j.joca.2018.04.009
[32] H.B. Menz, M. Marshall, M.J. Thomas, T. Rathod-Mistry, G.M. Peat, E. Roddy, Association between calcaneal enthesophytes and osteoarthritis of the hands and feet, Arthritis Care Res. 72 (2020) 1343–1348, https://doi.org/10.1002/acr.24.24030
[33] K.E. Kofman, A.H. Schuurman, M.C. Mulder, S.A.M.W. Verlinde, L.M. Gierman, P.J. Van Diest, et al., The pisotriquetral joint: osteoarthritis and enthesopathy, J. Hand Microsurg 6 (2014) 18–25, https://doi.org/10.1007/s12593-014-0129-3
[34] B. Moriggi, T. Kumai, S. Milz, M. Benjamin, The structure and histopathology of the “Enthesis organ” at the navicular insertion of the tendon of tibialis posterior, J. Rheuma 30 (2003) 508–517.
[35] J.J. Crisco, A.M. Morton, D.C. Moore, L.G. Kahan, A.L. Ladd, A.P.C. Weiss, Osteophyte growth in early thumb carpometacarpal osteoarthritis, Osteoarthr. Cartil. 27 (2019) 1315–1323, https://doi.org/10.1019/j.joca.2019.05.008
[36] S. Rein, E. Hagert, U. Hanisch, S. Lwowski, A. Fieguth, H. Zwipp, Immunohistochemical analysis of inter and intraligamentous distribution of sensory nerve endings in ankle ligaments: a cadaver study, Foot Ankle 34 (2013) 1017–1024, https://doi.org/10.1177/1071100713480862
[37] S. Rein, E. Hagert, U. Hanisch, S. Lwowski, A. Fieguth, H. Zwipp, Immunohistochemical analysis of sensory nerve endings in ankle ligaments: a cadaver study, Cells Tissues Organs 197 (2013) 64–76, https://doi.org/10.1159/000339877
[38] B.D. Stoeckl, K.M. Masada, L.G. Laforest, H.M. Lee, R.L. Mauck, D.R. Steinberg, Multi-scale analysis of regional pathology in the human trapezium during osteoarthritis progression, J. Orthop. Res. 43 (2025) 1581–1591, https://doi.org/10.1002/jor.26112
[39] A.T. Lee, A.A. Williams, J. Lee, R. Cheng, D.P. Lindsey, A.L. Ladd, Trapezium trabecular morphology in carpometacarpal arthritis, J. Hand Surg. Am. 38 (2013) 309–315, https://doi.org/10.1016/j.jhsa.2012.10.038
[40] P. Nufer, J. Goldhahn, T. Kohler, V. Kuhn, R. Müller, D.B. Herren, Microstructural adaptation in trapezial bone due to subluxation of the thumb, J. Orthop. Res. 26 (2008) 208–216, https://doi.org/10.1002/jor.20500